



Research Article

Green Synthesis of Piperine Loaded Gold/Triton X-100 Nanoconjugates: In-vitro Evaluation of Biocompatibility and Anti-Oxidant Activity

Muthusamy Prabakaran¹, Periakaruppan Nithya¹, Vellaikannu Kalaiarasi², Kalaivani Raman³, Susaimanickam Arul Antony^{1✉}, Mani Gajendiran^{3✉}

¹PG and Research, Department of Chemistry, Presidency College, Chennai 600005, India.

²Department of Chemistry, Karpaga Vinayaga College of Engineering and Technology, Palaynoor, Maduranthakam, Tamilnadu-603308, India.

³Department of Chemistry, School of Basic Sciences, Vels Institute of Science Technology and Advanced Studies (Vels University), Chennai 600117, India.

✉ Corresponding authors. E-mail: gajaunom@gmail.com or antonypresidency@gmail.com

Received: Nov. 25, 2018; **Accepted:** Jun. 9, 2019; **Published:** Jun. 21, 2019.

Citation: Muthusamy Prabakaran, Periakaruppan Nithya, Vellaikannu Kalaiarasi, Kalaivani Raman, Susaimanickam Arul Antony, and Mani Gajendiran, Green Synthesis of Piperine Loaded Gold/Triton X-100 Nanoconjugates: In-vitro Evaluation of Biocompatibility and Anti-Oxidant Activity. *Nano Biomed. Eng.*, 2019, 11(2): 192-199.

DOI: 10.5101/nbe.v11i2.p192-199.

Abstract

In this research, gold nanoparticles (Au NPs) were synthesized by a green chemical approach using the organic natural product piperine isolated from the black pepper. The piperine-Au NPs attached on the Triton X-100 and they were characterized by ultraviolet-visible absorption spectroscopy (UV-Vis), dynamic light scattering spectroscopy (DLS), X-ray powder diffraction (XRD), transmission electron microscopy (TEM), and energy dispersive X-ray spectroscopy (EDS). The TEM analysis confirmed the spherical shape of Au NPs with a diameter of 17-30 nm. The XRD analysis revealed that the Au NPs exhibited fcc crystal structure with an average crystallite size of 26 nm. The biocompatibility of the piperine-AuNPs-Triton X-100 nanoconjugates were examined on Hep-G2 cells. The piperine-AuNPs-Triton X-100 nanoconjugates exhibited better anti-oxidant activity.

Keywords: Gold nanoparticles; Piperine; Triton X-100; In vitro cytotoxicity; Anti-oxidant activity

Introduction

Gold nanoparticles (AuNPs) are of great interest in recent years due to their high surface area to volume ratio and their vast application in biomedical fields. They exhibit unusual properties such as optical, electrical, and catalytic properties because of their quantum confinement effect and the surface plasmon resonance (SPR) property. They are widely applied in enormous fields such as bio-sensing [1], optical

sensor [2], drug delivery [3-5], electronics [6], surface enhanced Raman spectroscopy (SERS) [7], biomarkers [8] and cancer treatment [9]. The physical and chemical properties of the AuNPs could easily be altered by changing the size and shape of the AuNPs, and hence they could easily be utilized for several applications [10, 11]. The chemically synthesized AuNPs usually produced toxic byproducts, and hence they could not be used for biomedical applications. The organic natural products isolated from various

plant extracts such as piperine, pectin, caffeine, and leucas aspera extract could act as reducing as well as stabilizing agent for the green synthesis of AuNPs or silver nanoparticles, and exhibited biocompatibility and biological activities [12-16].

The colloidal AuNPs stabilized with organic natural products in aqueous medium are much favored for several biomedical applications [13, 16, 17]. The AuNPs have been widely used to exhibit antibacterial activity against both Gram-positive and Gram-negative strains of bacteria [18]. The AuNPs have also been widely used in photothermal therapy for the treatment of cancer cells [19, 20]. The interest in treating the cancer cells using the plant extract-AuNPs nanoconjugates has been increasing in recent years because of their biocompatibility and effective anti-cancer activity. Anand et al. have reported the green synthesis of AuNPs using *Achyranthes aspera* Linn seed-epicotyls layer extracts, and that the nanoconjugates showed effective anticancer activity against cervical cancer cell lines [21].

The safrole present in black pepper could exhibit mild antioxidant and anti-carcinogenic effects. Natural products obtained from black pepper have been used for the treatment of constipation, diarrhea, hernia, indigestion, insect bites, and lung diseases [22, 23]. Synthesis of metal NPs by using medicinal plant extracts is a green approach and environmentally benign process. Even though the organic natural products act as both reducing as well as capping agent in the green synthesis of AuNPs, the shape and size of AuNPs may not be uniformly distributed. Hence, a biocompatible nontoxic polymer molecule is necessary to control the size and shape of the AuNPs. Triton-X100 is a non-ionic surfactant molecule, and it has been used as an efficient stabilizer for the synthesis of metal nanoparticles [16].

In the present study, we report the green synthesis of AuNPs using Triton X-100 as a stabilizer and piperine as a reducing agent. The gold nanoparticles were characterized by X-ray powder diffraction (XRD), transmission electron microscopy (TEM), energy-dispersive X-ray spectroscopy (EDS), ultraviolet-visible spectroscopy (UV-Vis), and Fourier transformed infrared spectroscopy (FTIR). The cytotoxicity of piperine-Triton X-100-AuNP nanoconjugates has been investigated on Hep-G2 cells, while the anti-oxidant activity of piperine-AuNPs has been investigated by DPPH assay.

Experimental Characterization techniques

The FTIR spectra of samples were recorded on a Perkin-Elmer FTIR spectrometer using KBr pellets. The UV-Vis spectra were recorded on a UV-visible absorption spectrophotometer (Perkin Elmer Lambda 35). The dynamic light scattering (DLS) spectra were recorded on a Malvern zeta sizer (Nano ZS). The TEM images were captured on FEI-TECNAI G2 (T-30) transmission electron microscope with an accelerating voltage of 250 kV. The XRD analyses were carried out on BRUKER D8 ADVANCE diffractometer with the monochromatic Cu-K α 1 radiation ($\lambda = 1.5418 \text{ \AA}$). The EDS analysis was carried out on a HITACHI SU6600 field emission scanning electron microscope (FESEM).

Materials

Auric chloride and Triton X-100 of analytical grade were procured from Sigma Aldrich. Piperine was isolated from black pepper powder as given in our earlier work [16].

Synthesis of gold nanoparticles

5 gm of piperine powder was dispersed in 50 mL of DD water, and it was centrifuged at 10000 rpm for 10 min. The resultant clear solution was used for the synthesis of gold nanoparticles at different concentrations using Triton X-100 (0.6 mL) as the surfactant. The main role of the Triton X-100 was to act as a shape control of AuNPs. Piperine (2.5 mL) (0.1-0.5%) was added to 50 mL of aqueous auric chloride solution (1 mM), and the solution mixture was heated to 90 °C until the formation of wine-red color.

Cell viability assay

The cytotoxicity of synthesized nanoconjugates towards Hep-G2 cells were tested by in-vitro cell culture method [16]. Hep-G2 cells were cultured in a 96-well culture plate and samples at different concentrations (10, 25, 50, 100 and 250 $\mu\text{g/mL}$) were added. After incubation for 24 h, MTT assay was performed to determine cell viability percentage as given in literature [16].

DPPH free radical scavenging assay

DPPH radical scavenging activity of the nanoconjugates was determined by following a literature procedure [24]. Briefly, an aliquot of 0.5 mL of sample solution in methanol was mixed with 2.5 mL of 0.5 mM methanolic solution of DPPH [24].

The mixture was shaken vigorously and incubated for 30 min in the dark at room temperature. The absorbance was measured at 517 nm using a UV spectrophotometer. Ascorbic acid was used as a positive control. DPPH free radical scavenging ability (%) was calculated by using the formula:

$$\% \text{ of inhibition} = \frac{\text{absorbance of control} - \text{absorbance of sample}}{\text{absorbance of control}} \times 100.$$

Results and Discussion

Fourier transformed infrared spectroscopy

Fig. 1(a) and (b) show the FTIR spectra of pure piperine and piperine-AuNPs nanoconjugates respectively. The major stretching frequencies in the spectrum of piperine were observed at 2926, 2912, 1705, 1653, 1547, 1475, 1357, 1237 and 1023 cm^{-1} (Fig. 1(a)), while the piperine capped AuNPs showed characteristic stretching frequencies at 2938, 2852, 1633, 1582, 1490, 1449, 1239, 1193, 1133 and 1029 cm^{-1} (Fig. 1(b)) [25]. The bands observed at 2926 cm^{-1} corresponded to an asymmetric C–H stretching frequency, while the signal at 1705 cm^{-1} corresponded to a carbonyl stretching vibration. The signals appeared at 1239 and 1240 cm^{-1} were due to the presence of C–O stretching vibration of alcohol group.

In the case of FTIR spectrum of piperine-AuNPs, the carbonyl stretching frequency of piperine at 1705

cm^{-1} shifted to 1633 cm^{-1} , which indicated that the carbonyl group of piperine involved in reduction of Au^{3+} to Au^0 . A shift in the peaks of the FTIR spectrum of piperine capped AuNPs was observed from 2926 to 2938 cm^{-1} , 1705 to 1633 cm^{-1} , and the remaining peaks were unchanged suggesting the binding of AuNPs with piperine molecule.

Ultraviolet-visible spectroscopy and dynamic light scattering

UV-Vis is a useful technique to determine the size and stability of nanoparticles. Formation of AuNPs was confirmed primarily by UV-Vis. The color change was attributed to the surface plasmon resonance (SPR) phenomenon. The UV-visible absorption spectra showed an absorption maximum in the wavelength range of around 530–557 nm as evident from Fig. 2(a) corresponding to the SPR band for AuNPs [14]. An absorption signal at 340–360 nm corresponded to the absorption of piperine, and this signal shifted towards red region with increased concentration of piperine [26]. These UV-visible spectral results confirmed the conjugation of piperine with AuNPs. When the concentration of piperine was increased from 0.1 to 0.5%, the SPR signal of AuNPs also increased with a slight shift towards higher wavelength region (Fig. 2). When the concentration of piperine was increased to above 0.5%, the absorbance remained constant without any further increment. These results

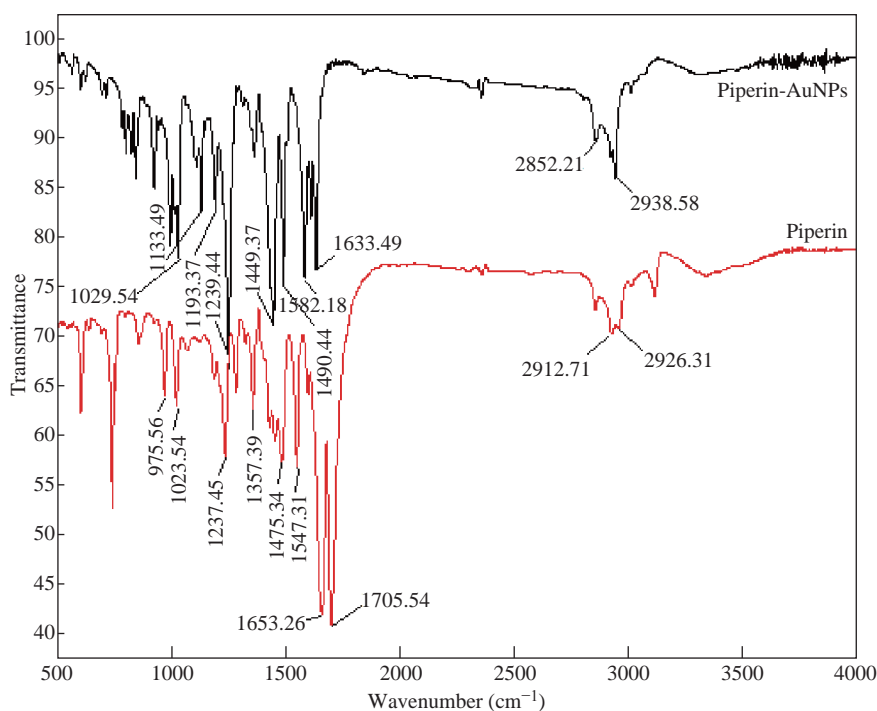


Fig. 1 Fourier transform infrared spectra of (a) piperine, and (b) piperine-AuNPs.

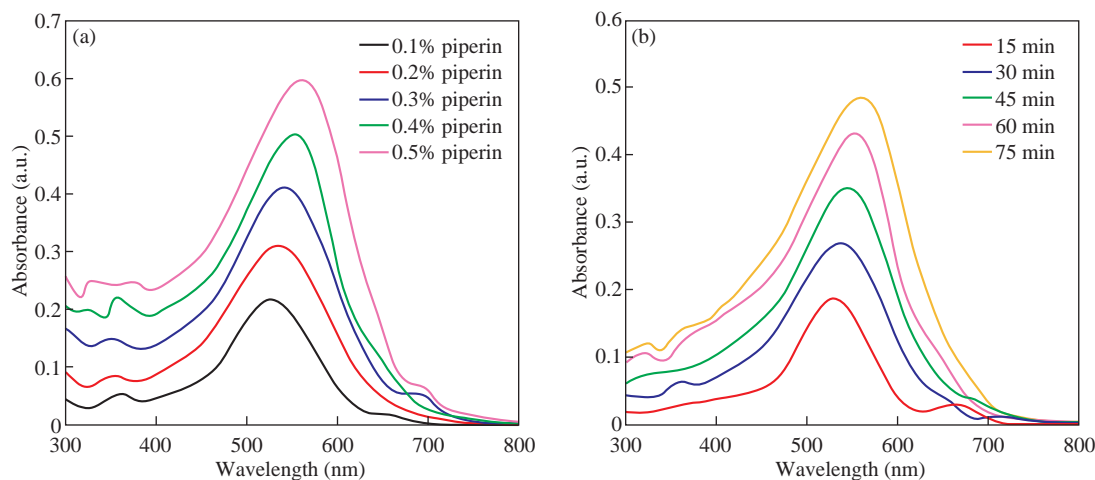


Fig. 2 Absorption spectra of (a) different concentrations of piperine-AuNPs solutions, and (b) recorded at different time intervals of piperine-AuNPs solutions.

suggested that 2.5 mL of piperine (0.5%) was required to reduce 50 mL of aqueous auric chloride solution (1 mM), and the piperine effectively reduced Au^{3+} to Au^0 and conjugated to AuNPs. The UV-visible spectra of AuNPs synthesized with fixed concentration of piperine at different time intervals (15, 30, 45, 60, and 75 min) were recorded (Fig. 2(b)). The SPR signal increased with the time increasing up to 75 min, which indicated that the overall reaction time was 75 min for complete reduction of Au^{3+} ions to Au^0 . The formation of AuNPs started within 15 min, and then the peak intensity increased up to 75 min (Fig. 2(b)). After 75 min of the reaction, all the Au^{3+} were reduced to Au^0 ; hence the absorbance intensity was constant. It suggested that the reduction of Au^{3+} to AuNPs required 75 min for 100% completion of the reaction at the specified reaction conditions.

The DLS spectral technique was used to determine the average particle size of the synthesized AuNPs. The piperine capped AuNPs-Triton X-100 nanoconjugates exhibited two peaks at 33 and 250 nm corresponding to AuNPs and Triton X-100 polymer, respectively (Fig. 3(b)). The AuNPs free Triton X-100 exhibited only one peak at 300 nm, and these results confirmed the formation of AuNPs stabilized by Triton X-100 polymer (Fig. 3(a)).

Transmission electron microscopy and energy-dispersive X-ray spectroscopy

The TEM images of piperine-AuNPs are shown in Fig. 3(a)-(c). The AuNPs exhibited a spherical shape with an average size of 28 nm, and this result agreed with the DLS spectral result (Fig. 4). TEM results suggest that the piperine capped AuNPs were not

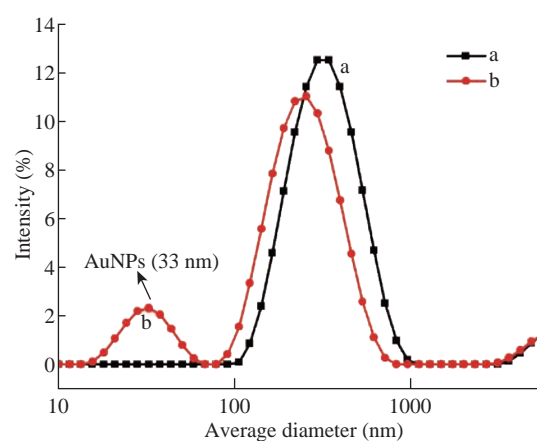


Fig. 3 DLS spectra of (a) piperine-Triton X-100 mixture, and (b) piperine-AuNPs-Triton X-100 nanoconjugates.

agglomerated.

The elemental composition of the as-prepared piperine-AuNPs was determined through EDS. The EDS spectrum showed a peak of Au at 2.1 keV (Fig. 5). The EDS spectrum also showed the signals of C and O atoms, which confirmed the functionalization of piperine on gold nanoparticles.

X-ray powder diffraction

The XRD pattern of the piperine-AuNPs showed four main characteristic Bragg diffraction peaks positioned at 2θ values of 19.14, 23.47, 38.33, 44.61 and 64.80° (Fig. 6). The X-ray diffraction signals corresponded to (111), (200) and (220) facets of fcc crystal structure of AuNPs. The diffraction peaks were consistent with standard database files (JCPDS card No 04-0784), indicating that the synthesized AuNPs were of fcc crystalline nature [27]. Size of the piperine-AuNPs was evaluated from the XRD data using the

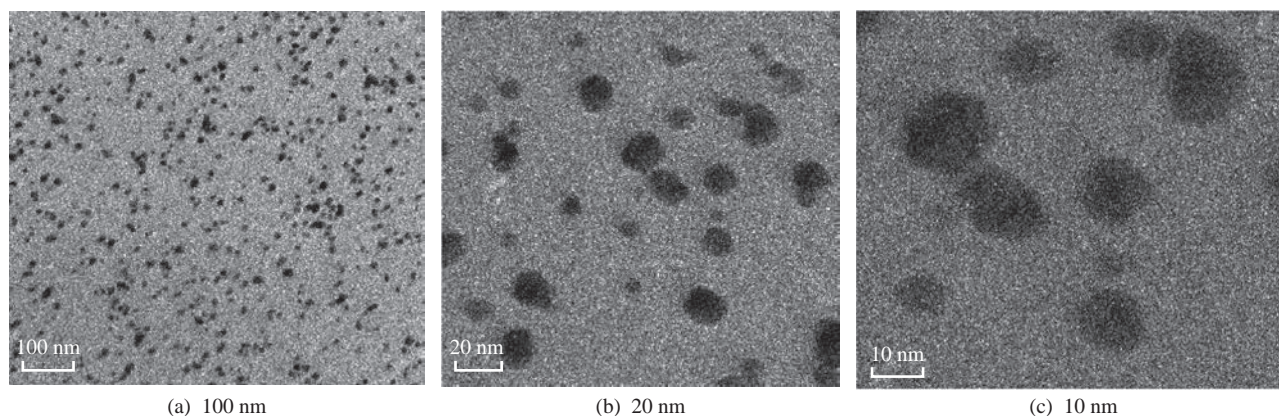


Fig. 4 (a)-(c) Transmission electron microscopy images of piperine-AuNPs-Triton X-100 nanoconjugates.

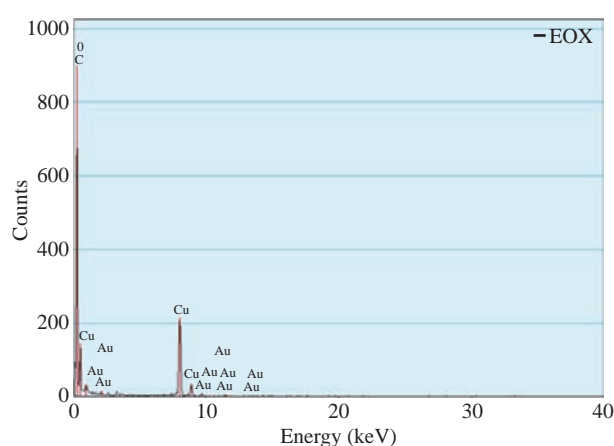


Fig. 5 The energy dispersive X-ray analysis of Piperine/Triton X-100/AuNPs.

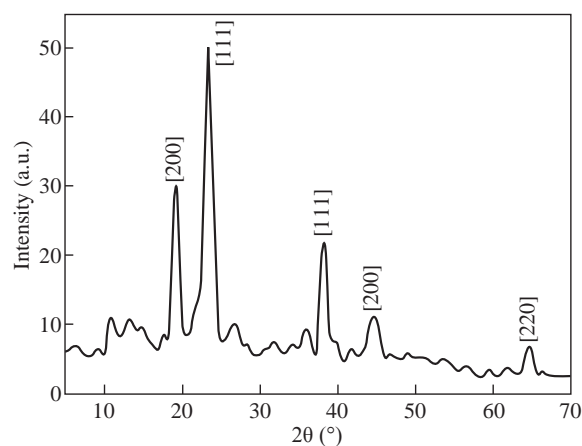


Fig. 6 The X-ray powder diffraction spectrum of Piperine-AuNPs-Triton X-100.

Debye-Scherrer equation, $d = k\lambda/\beta\cos\theta$. The crystallite size was determined to be 26 nm, and it was consistent with TEM results.

Cell viability assay

The use of nontoxic nanoparticles with biocompatible capping materials is an important aspect in biomedical applications. Fig. 7 shows the viability of Hep-G2 cells in various concentrations of

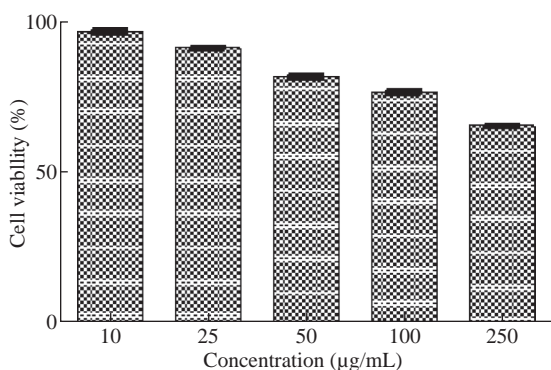


Fig. 7 The cell viability of Hep-G2 cancer cell lines in various concentrations of piperine-AuNP-Triton X-100.

AuNPs (10-250 µg), and showed excellent viability up to 100 µg/mL of AuNPs. This indicated that the piperine-Triton X-100 provided a nontoxic coating on the surface of AuNPs. It revealed that the synthesized AuNPs were of insignificant toxicity on Hep-G2 cells, providing an opportunity for their application in drug delivery.

Fig. 8 shows the cellular morphologies of Hep-G2 cells treated with different concentrations of piperine-AuNPs, and it suggested that treatment with piperine-AuNPs did not induce any cytotoxic effect and they did not show significant damage or death of the treated cells.

Antioxidant activity by DPPH assay

The radical-scavenging activity of piperine-AuNPs was performed by following a literature procedure [24]. As shown in Fig. 9, all AuNPs scavenged DPPH radicals in a dose-dependent manner and shared a good linear correlation between the percentage inhibition of the DPPH and the concentration of AuNPs. The percentage inhibition of DPPH ranged from about 18%

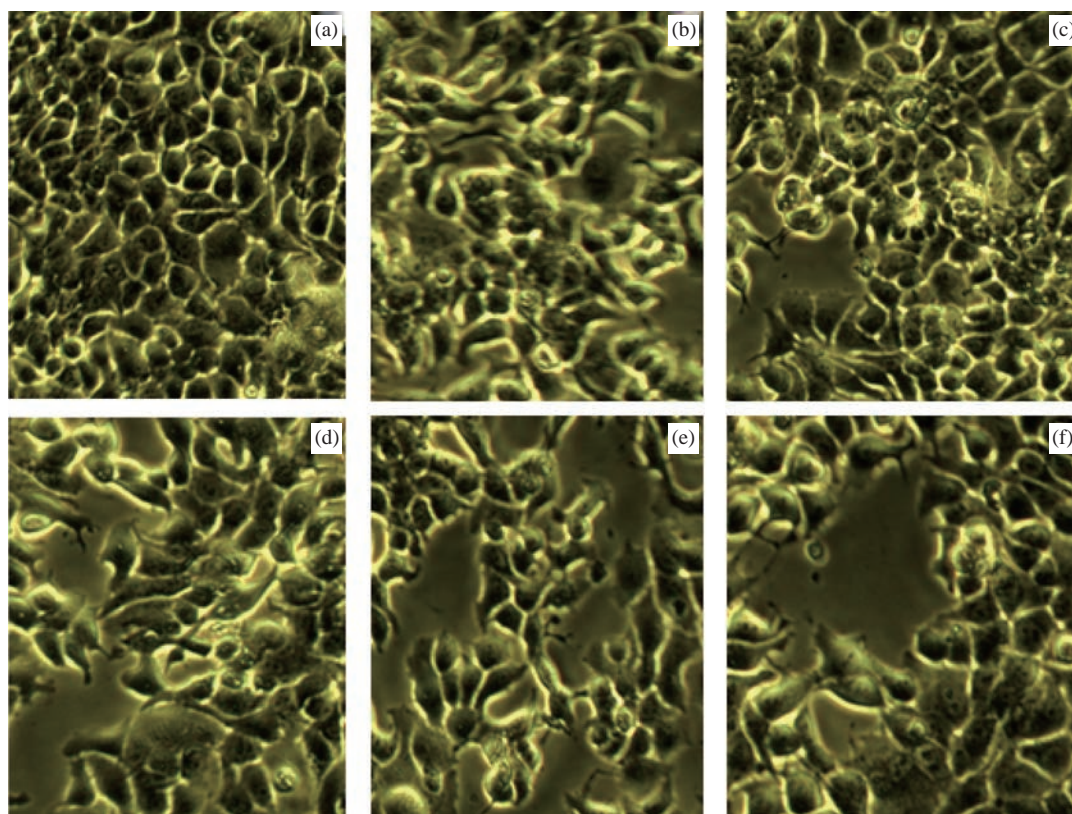


Fig. 8 The cellular morphologies of Hep-G2 cells treated with piperine-AuNPs at (a) 0, (b) 10, (c) 25, (d) 50, (e) 100 and (f) 250 µg/mL.

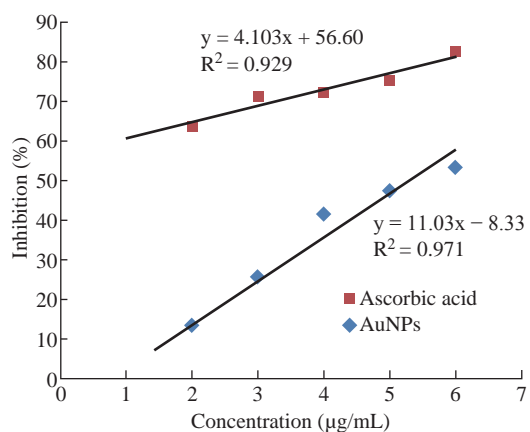


Fig. 9 The linear correlation between the percentage inhibition of the DPPH and the concentration of piperine-AuNPs.

at a lower concentration (10 µg/mL) to 53% obtained at a higher concentration (250 µg/mL) of piperine-AuNPs.

Fig. 10 revealed the existence of effective radical scavenging activity of piperine extract and biosynthesized AuNPs when compared with the standard ascorbic acid. The highest radical scavenging activity with 53% was observed in AuNPs at 250 µg/mL. The DPPH radical scavenging activities of piperine-AuNPs increased gradually in a dose dependent manner (from 10 to 250 µg/mL). Similar

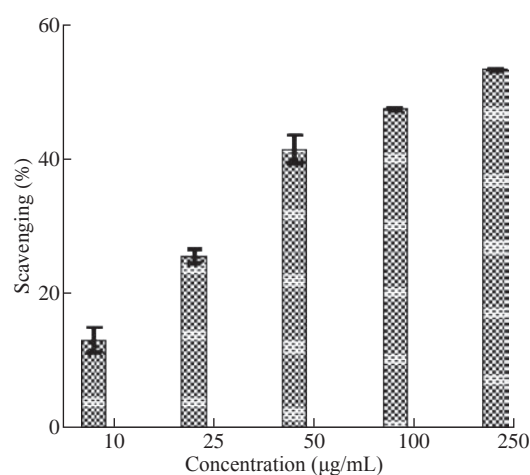


Fig. 10 DPPH radicals scavenging activity of piperine-AuNPs. (Values were calculated by comparison with ascorbic acid's radical scavenging activity.).

results were obtained for *I. herbstii* aqueous leaf extract [28].

The DPPH values increased in a dose dependent manner. The recorded value for the lowest concentration of the piperine extract 10 µg/mL was 13.28±3.24, and this value increased to 53.47±0.24. When the concentration was increased up to 250 µg/mL of the piperine-AuNPs, there was a higher level of scavenging activity.

Conclusions

Triton X-100 as a nonionic surfactant, piperine and auric chloride was successfully used for the green synthesis of AuNPs. The piperine was isolated from the black pepper and characterized by the FTIR and UV-Vis. Triton X-100 acted as a stabilizing agent, while piperine acted as a reducing agent. The UV-visible absorption spectra exhibited a maximum absorption at 530-557 nm, while the DLS spectral analysis showed 33 nm of average diameter of Triton X-100 stabilized piperine-AuNPs. The TEM analysis confirmed that the AuNPs showed a spherical shape with 28 nm of size. The in-vitro cytotoxicity results showed that the piperine-AuNPs nanoconjugates were not toxic up to 50 µg/mL, while they showed moderate toxicity at 250 µg/mL towards Hep-G2 cells. The piperine-AuNPs system showed potential anti-oxidant activity compared with the standard ascorbic acid. Hence, the developed piperine-AuNPs-Triton X-100 system could be used as an anti-oxidant agent.

References

- [1] T.S. Lai, T.C. Chang, and S.C. Wang, Gold nanoparticle-based colorimetric methods to determine protein contents in artificial urine using membrane micro-concentrators and mobile phone camera. *Sensors and Actuators, B: Chemical*, 2017, 239: 9-16.
- [2] M.M. Ayad, H.E. Abdellatef, M.M. Hosny, et al., Spectrophotometric determination of etilefrine HCl, salbutamol sulphate and tiemonium methyl sulphate using surface Plasmon resonance band of gold nanoparticles. *Nano Biomedicine and Engineering*, 10, 2018: 16-24.
- [3] P. Manivasagan, S. Bharathiraja, N.Q. Bui, et al., Paclitaxel-loaded chitosan oligosaccharide-stabilized gold nanoparticles as novel agents for drug delivery and photoacoustic imaging of cancer cells. *International Journal of Pharmaceutics*, 511, 2016: 367-379.
- [4] G. Mani, S. Kim, and K. Kim, Development of folate-thioglycolate-gold nanoconjugates by using citric acid-PEG branched polymer for inhibition of MCF-7 cancer cell proliferation. *Biomacromolecules*, 2018, 19: 3257-3267.
- [5] M. Gajendiran, P. Balashanmugam, P.T. Kalaichelvan, et al., Multi-drug delivery of tuberculosis drugs by π -back bonded gold nanoparticles with multiblock copolyesters. *Materials Research Express*, 2016, 3: 065401.
- [6] S. Mahendia, P.K. Goyal, A.K. Tomar, et al., Study of dielectric behavior and charge conduction mechanism of poly(vinyl alcohol) (PVA)-copper (Cu) and gold (Au) nanocomposites as a bio-resorbable material for organic electronics. *Journal of Electronic Materials*, 2016, 45: 5418-5426.
- [7] R.M. West, S. Semancik, Interpenetrating polyaniline-gold electrodes for SERS and electrochemical measurements. *Applied Surface Science*, 2016, 387: 260-267.
- [8] A. Zhang, C. Huang, H. Shi, et al., Electrochemiluminescence immunosensor for sensitive determination of tumor biomarker CEA based on multifunctionalized Flower-like Au@BSA nanoparticles. *Sensors and Actuators, B: Chemical*, 2017, 238: 24-31.
- [9] R. Hoshyar, G.R. Khayati, M. Poorgholami, et al., A novel green one-step synthesis of gold nanoparticles using crocin and their anti-cancer activities. *Journal of Photochemistry and Photobiology B: Biology*, 2016, 159: 237-242.
- [10] X. Lu, A. Dandapat, Y. Huang, et al., Tris base assisted synthesis of monodispersed citrate-capped gold nanospheres with tunable size. *RSC Advances*, 2016, 6: 60916-60921.
- [11] S. Manju, B. Malaikozhundan, and S. Vijayakumar, Antibacterial, antibiofilm and cytotoxic effects of Nigella sativa essential oil coated gold nanoparticles. *Microbial Pathogenesis*, 2016, 91: 129-135.
- [12] C. Wang, R. Mathiyalagan, and Y.J. Kim, Rapid green synthesis of silver and gold nanoparticles using Dendropanax morbifera leaf extract and their anticancer activities. *International Journal of Nanomedicine*, 2016, 11: 3691-3701.
- [13] K. Reena, M. Prabakaran, B. Leeba, et al., Green synthesis of pectin-gold-PLA-PEG-PLA nanoconjugates: In vitro cytotoxicity and anti-inflammatory activity. *Journal of Nanoscience and Nanotechnology*, 2017, 17: 4549-4557.
- [14] R. Kamalakannan, G. Mani, P. Muthusamy, et al., Caffeine-loaded gold nanoparticles conjugated with PLA-PEG-PLA copolymer for in vitro cytotoxicity and anti-inflammatory activity. *Journal of Industrial and Engineering Chemistry*, 2017, 51: 113-121.
- [15] K. Reena, P. Balashanmugam, M. Gajendiran, et al., Synthesis of leucas aspera extract loaded gold-PLA-PEG-PLA amphiphilic copolymer nanoconjugates: In vitro cytotoxicity and anti-inflammatory activity studies. *Journal of Nanoscience and Nanotechnology*, 2016, 16: 4762-4770.
- [16] M. Prabakaran, V. Kalaiarasi, P. Nithya, et al., Green synthesis of Piperine/Triton X-100/ silver nanoconjugates: Antimicrobial activity and cytotoxicity. *Nano Biomedicine and Engineering*, 2018, 10: 141-148.
- [17] S. Balasubramanian, S.M.J. Kala, T.L. Pushparaj, et al., Biofabrication of gold nanoparticles using Cressa cretica leaf extract and evaluation of catalytic and antibacterial efficacy. *Nano Biomedicine and Engineering*, 2019, 11: 58-66.
- [18] E.A. Siddiqui, A. Ahmad, A. Julius, et al., Biosynthesis of anti-proliferative gold nanoparticles using endophytic Fusarium oxysporum strain isolated from neem (A. indica) leaves. *Current Topics in Medicinal Chemistry*, 2016, 16: 2036-2042.
- [19] M.R.K. Ali, H.R. Ali, C.R. Rankin, et al., Targeting heat shock protein 70 using gold nanorods enhances cancer cell apoptosis in low dose plasmonic photothermal therapy. *Biomaterials*, 2016, 102: 1-8.
- [20] S. Abbasi, M. Servatkah, and M.M. Keshtkar, Advantages of using gold hollow nanoshells in cancer photothermal therapy. *Chinese Physics B*, 2016, 25: 087301.
- [21] M. Anand, V. Selvaraj, M. Alagar, et al., Green phyto-synthesis of gold nanoparticles using Achyranthes aspera Linn seed-epicotyls layer extracts and its anticancer activity. *Asian Journal of Pharmaceutical and Clinical Research*, 2014, 7: 136-139.
- [22] S.H. Lee, H.Y. Kim, S.Y. Back, et al., Piperine-mediated drug interactions and formulation strategy for piperine: recent advances and future perspectives. *Expert Opinion on Drug Metabolism and Toxicology*, 2018, 14: 43-57.
- [23] P.D.A. Oliveira, T.B. de Almeida, R.G. de Oliveira, et al., Evaluation of the antinociceptive and anti-inflammatory activities of piperic acid: Involvement of

- the cholinergic and vanilloid systems. *European Journal of Pharmacology*, 2018, 834: 54-64.
- [24] İ. Gülçin, Antioxidant properties of resveratrol: A structure–activity insight. *Innovative Food Science & Emerging Technologies*, 2010, 11: 210-218.
- [25] P.R.D. Swapna, V. Junise, P. Shubin, et al., Isolation, identification and antimycobacterial evaluation of piperine from Piper longum. *Der Pharmacia Lettre*, 2012, 4: 863-868.
- [26] N.K. Singh, P. Kumar, and D.K. Gupta, UV-spectrophotometric method development for estimation of piperine in Chitrakadi Vati. *Der Pharmacia Lettre*, 2011, 3: 178-182.
- [27] X. Ren, Y. Song, and A. Liu, Experimental and theoretical studies of DMH as a complexing agent for a cyanide-free gold electroplating electrolyte. *RSC Advances*, 2015, 5: 64997-65004.
- [28] C. Dipankar, S. Murugan, The green synthesis, characterization and evaluation of the biological activities of silver nanoparticles synthesized from Iresine herbstii leaf aqueous extracts. *Colloids and Surfaces B: Biointerfaces*, 2012, 98: 112-119.

Copyright© Muthusamy Prabakaran, Periakaruppan Nithya, Vellaikannu Kalaiarasi, Kalaivani Raman, Susaimanickam Arul Antony, and Mani Gajendiran. This is an open-access article distributed under the terms of the Creative Commons Attribution License, which permits unrestricted use, distribution, and reproduction in any medium, provided the original author and source are credited.